SWASH ZONE MORPHODYNAMICS OF COARSE-GRAINED BEACHES DURING ENERGETIC WAVE CONDITIONS

Luis Pedro Almeida[1], Gerd Masselink[1], Paul Russell[1], Mark Davidson[1], Robert McCall[1] and Tim Poate[1],

A 2D laser-scanner was deployed on four different coarse-grained beaches (Chesil, Loe Bar, Hayling Island and Seascale – all in UK) to measure the swash morphodynamics during energetic wave conditions (offshore H_s > 2m). Field observations performed with the laser-scanner showed that different types of coarse-grained beaches present contrasting morphological responses under energetic hydrodynamics. The surf scaling parameter, a proxy of the morphological condition and wave steepness on the swash, showed an inverse relationship with the extreme vertical runup illustrating that runup is enhanced by low steepness swell waves for a given coarse-grained beach\slope; nevertheless additional parameters are needed to explain the entire runup variability.

Keywords: coarse-grained beaches; swash zone; wave runup; morphodynamics; laser-scanner.

Introduction

Coarse grained beaches are common along high latitudes (e.g., Canada, UK, and Ireland) and at many locations elsewhere, although on a world-wide scale they are relatively scarce. The composition, size and form of theses beaches varies widely; however, according to Jennings and Schulmeister (2002) they can be classified into three categories: (1) pure gravel beaches (PG), composed of particle size ranging from fine gravel to coarse pebbles, with minimal sand; (2) mixed sand-gravel beaches (MSG), with high proportions of both coarse particles and sand, with there being an intimate mixing of the two size fractions in the beach deposit; and (3) composite sand-gravel beaches (CSG), with an upper foreshore composed of gravel and cobbles, and a lower foreshore of sand, generally with a distinct boundary between them.

The vast majority of research into the swash morphodynamics of coarse-grained beaches has been concerned with PG beaches, particularly of relatively small-scale processes during mild wave conditions (e.g., Horn et al., 2003; Austin and Masselink, 2006; Ivamy and Kench, 2006; Pedrozo-Acuña et al., 2006; Austin and Buscombe, 2008; Masselink et al., 2010) and, more recently, during energetic wave conditions (Poate et al., 2013; Almeida et al., 2014). Typically PG beaches are different in form to MSG and CSG, and the morphodynamics of MSG and CSG are distinct and potentially more complex than either pure sand (PS) or PG beaches (Kirk, 1970; Jennings and Shulmeister, 2002; Kulkarni et al., 2004; Pontee et al., 2004; Ivamy and Kench, 2006). There is further evidence to suggest that the hydrodynamic regimes and morphological response on MSG and CSG beaches will be different from PG and PS beaches, largely due to the differences in the transport and permeability characteristics of sand and gravel (Pontee, *et al.*, 2004).

Sand is moved predominantly by saltation and suspension, by both currents and waves, while gravel is moved by sliding and rolling (and saltation to a lesser extend) largely by waves (Carter and Orford, 1984). Thus, gravel has a propensity for onshore movement due to its high threshold of motion and the asymmetry swash zone action (Carr, 1983). Sand, on the other end, can move onshore or offshore under wave action.

The higher permeability of PG beaches encourages swash infiltration and this forms the basis for the mechanism of slope development under swash asymmetry. On PS beaches the swash infiltration mechanism responsible for onshore swash transport is considered to be insignificant due to the low levels of infiltration (Masselink and Li, 2001). On MSG and CSG beaches, the water table response is controlled by the underlying content of sand, which can lead to a similar behaviour to a PS beach and the development of lower slopes (Orford, 1984). While steep berms can form on PG beaches, the higher hydraulic conductivity permits greater energy dissipation than occurs on similarly steep MSG, where even 20% sand content reduces the hydraulic conductivity by an order of magnitude (Mason *et al.*, 1997).

The hydraulically-rough and permeable nature of the coarse sediments (D > 2 mm), together with their ability to develop a steep beach-face (reflective) provide to coarse-grained beaches efficient mechanisms for wave energy dissipation and therefore natural means of coastal defence (Carter and

[1] School of Marine Sciences and Engineering, University of Plymouth, Drake Circus, Plymouth, Devon, PL4 8AA, United Kingdom

Orford, 1993; van Wellen *et al.*, 2000; Buscombe and Masselink, 2006; Moses and Williams, 2008). These aspects have raised a recent interest in these environments for engineering applications such as beach nourishment (e.g., Moses and Williams, 2009); however, there are important limitations in understanding the behaviour of these beaches under energetic wave conditions (i.e., storms). The lack of field measurements provides the main reason for this knowledge a gap and stems from the lack of suitable instruments capable of making direct measurement in an energetic swash zone in which large clasts are moving and where significant morphological changes occur in a very short period of time (Osborne, 2005).

Remote sensing methods emerge in this context as the most appropriate solution for this type of field measurement, and recent developments on the use of 2D laser-scanners (Blenkinsopp et al., 2010, 2012; Brodie et al., 2012; or Almeida et al., 2013) to perform high frequency measurements of swash zone dynamics (including morpho and hydrodynamics) have demonstrated to be one of the most adequate tool for this propose.

In line with these aforementioned justifications the aim of present work is to improve the understanding of swash zone morphodynamics of coarse-grained beaches during energetic wave conditions using field measurements performed with a 2D laser-scanner. To accomplish this, four field experiments were performed on different coarse-grained beaches during energetic wave conditions (H_s > 2 m). The unique datasets were analysed to characterize and compare the gravel beach morphological responses and hydrodynamics characteristics during such specific conditions.

Methods

Four field experiments were conducted between March 2012 and October 2013 at four different coarse-grained beaches: 1) Chesil in Dorset – coarse PG; 2) Loe Bar in Cornwall – fine PG; 3) Hayling Island in Hampshire – CSG beach; and 4) Seascale in Cumbria – MSG beach. Figure 1 shows the location of each site and a sketch of the type of beach profile, while information about the tide regime, wave climate, sediment size and survey dates is presented in Table 1.

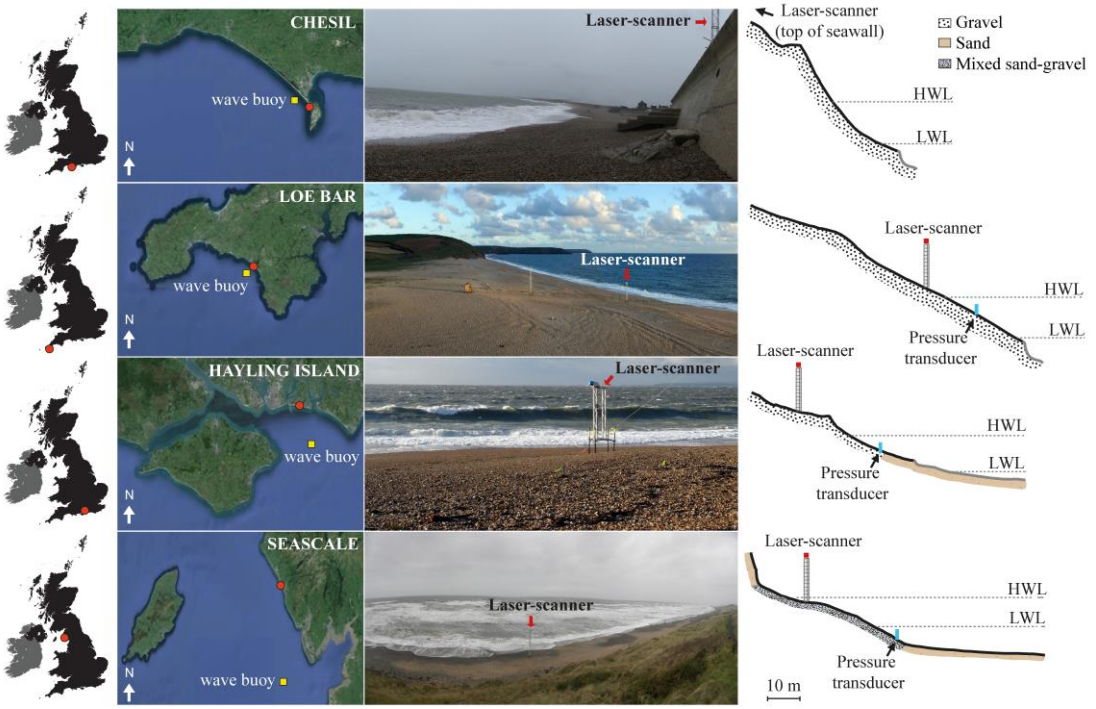

Figure 1. Study site locations, field photo and sketch of the type of beach profile showing shape, composition, location of the instrumentation and highest and lowest water level (HWL and LWL) observed during the field experiments.

Chesil beach – coarse PG

Chesil beach is a long (18 km) linear coarse PG beach that extends from Abbotsbury in the west, to Chesilton in the east where it is backed by a seawall (Figure 1). With a systematic long-shore size-grading, the mean size of the pebbles increases from the west (D_{50} = 25 mm at Herbury Point) towards

the east, Chesilton (D_{50} = 50 mm), while beach width decreases from west (150 to 200 m wide) to east, reducing to a width of 40–60 m at its eastern end (Carr, 1969). The present deployment was performed at the eastern end of Chesil beach, in front of the seawall, where the beach profile is characterised by a narrow berm attached to the toe of the structure and a very steep beach face with a pronounced beach step at the bottom of the profile (Figure 1). The mean spring tidal range at Bridport is 3.5 m and waves from the south-west have an average annual significant height around 1 m with 8 seconds of peak period (Table 1).

Loe Bar – fine PG

Loe Bar is part of a 4.3-km long gravel beach (D_{50} = 2–4 mm) that extends from Porthleven, in the north, to Gunwalloe, in the south (Figure 1). Loe Bar barrier fronts Loe Pool and extends 430 m between the adjacent headlands, with an average width of 200 m and a typical seaward gradient of 0.1. With a NW-SE shoreline orientation, the barrier faces south-west and is exposed to energetic Atlantic swell with an annual average significant wave height (H_s) of 1.2 m, an average peak period (T_p) of 9.1 s and a direction (θ) of SW (Table 1 - Poate *et al*., 2013). The tidal regime is macro-tidal with a mean spring tidal range of 4.5 m.

Hayling Island - CSG

Hayling Island is a CSG beach located in the East Solent and forms part of the much larger Solent estuarine system. The beach runs from the entrance to Langstone Harbour in the west, to Chichester Harbour in the east, over a distance of approximately 6 km. West of Chichester Harbour, for about 2 km, the beach is relatively narrow and many groynes have been constructed over the years to deal with erosion and flooding problems (Whitcombe, 1996). To the west of this area, the beach is much wider and unprotected, and this is where the field experiment was undertaken. At this location the beach profile presents a steep upper foreshore composed of coarse gravel (D_{50} = 16 mm) and a gently sloping sandy lower foreshore exposed at low water. The mean spring tidal range is 4.6 m and due to the shelter provided by the Isle of Wight the mean annual significant wave height of this area is only 0.7 m with peak periods of 7.6 s (Table 1).

Seascale - MSG

Seascale is a MSG beach located on the Cumbria coastline and part of a 9-km (from Ravenglass, in the south, to Sellafield, in the North) coastal segment (Figure 1). This coastal section is formed by a high frontal dune ridge (approximately 10 m high) except in the front of the village of Seascale, where the dune ridge is absent and instead is occupied by human infrastructures (houses, car park, seawall). The foreshore is composed of a narrow (between 50 to 70 m) and low gradient mixed sand and gravel beach face (gravel size varies between D_{50} = 2 to 60 mm; and sandy with D_{50} = 0.24 mm) fronted by a very large sandy intertidal terrace (approximately 500 m wide) with irregularly spaced patches of boulders. The mean spring tidal range is 7 m and the mean annual significant wave height of this area is approximately 1 m with peak periods of 7 s (Table 1).

Table 1. Wave climate, tides and sediment characteristics of the study sites.

	Chesil	Loe Bar	Hayling Island	Seascale
Survey dates	16 and 17 December 2012	23, 24 and 25 March 2012	27 and 28 October 2013	From 28 and 29 January 2013
Spring Tidal range (m)	3.5	4.5	4.6	7
Mean annual H_s (m)	1	1.2	0.7	1
Mean annual T_p (s)	8	9.1	7.6	3.5
Mean annual θ (quad)	SW	SW	S	SW
D_{50} (mm)	50	2 to 4	16 (gravel) and 0.15 (sand)	2 to 60 (gravel) and 0.24 (sand)

Field experiments were performed during energetic wave conditions (H_s > 2 m) and measurements included the characterization of the offshore and inshore wave conditions (obtained from the offshore wave buoys and inshore pressure transducers deployed at each site – the only exception was the absence

of an inshore PT at Chesil beach) and high frequency swash morphological changes and hydrodynamics measured with a 2D laser-scanner (Figure 1).

The LD-OEM3100 (manufactured by SICK) laser scanner model was selected for the present work. This model is a two-dimensional mid-range (maximum range ≈ 100 m; SICK, 2009) laser-scanner that emits pulsed laser beams (invisible infrared light; λ = 905 nm) that are deflected on an internal mirror (inside the scanner head) that rotates at regular angular steps and scans the surroundings (360°) in a circular manner (Figure 2). The scanner head rotates at 2.5 Hz with an angular resolution of 0.125° and the distance to the target is calculated from the propagation time that the light requires from emission to reception of the reflection at the sensor. The instrument is mounted on top of an aluminium tower attached to a scaffold base inserted into the each, allowing the coverage of a c. 60-m cross-shore section of the beach profile (Figure 1 and 2).

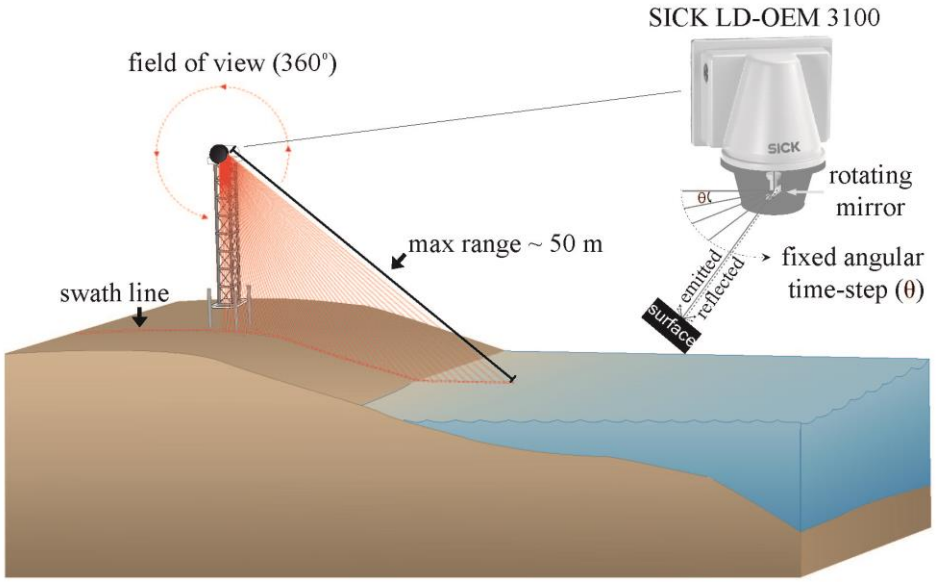

Figure 2. Sketch of the 2D laser-scanner deployment and working principles.

The measurements are logged at 2.5 Hz and consist of two dimensional polar coordinates (d_i, α_i), where i is the scan number (complete cycle of scanner field of view), d is the distance measured between the laser-scanner and the target and α is the relative angle of the measurement. Laser polar measurements (d_i, α_i) are initially converted to Cartesian coordinates (x_i, z_i), where x is the cross-shore position and z elevation, by applying a polar transformation. This new coordinate system is referred to a local coordinate system, where the cross-shore origin (x = 0) is at the top of the beach and the vertical datum is referred to the Ordnance Datum of Newlyn (ODN - 0 m ODN ~ 0.2 m above mean sea level). Measurements performed with the laser-scanner were corrected to compensate for levelling and orientation errors, and a variance threshold was applied to separate the beach topography from the water motions, following the method proposed by Almeida *et al.* (2013).

After this initial data processing, the laser measurements are separated in two distinct time series (Figure 3): (1) continuous beach topography and (2) swash hydrodynamics (including water elevation and runup edge). These time series form the basis of the analysis of the present work. This data analysis method allows the complete coverage of the swash zone with a vertical accuracy of approximately ±1.5 cm and horizontal resolutions that range from millimetres to centimetres (Almeida *et al.*, 2014).

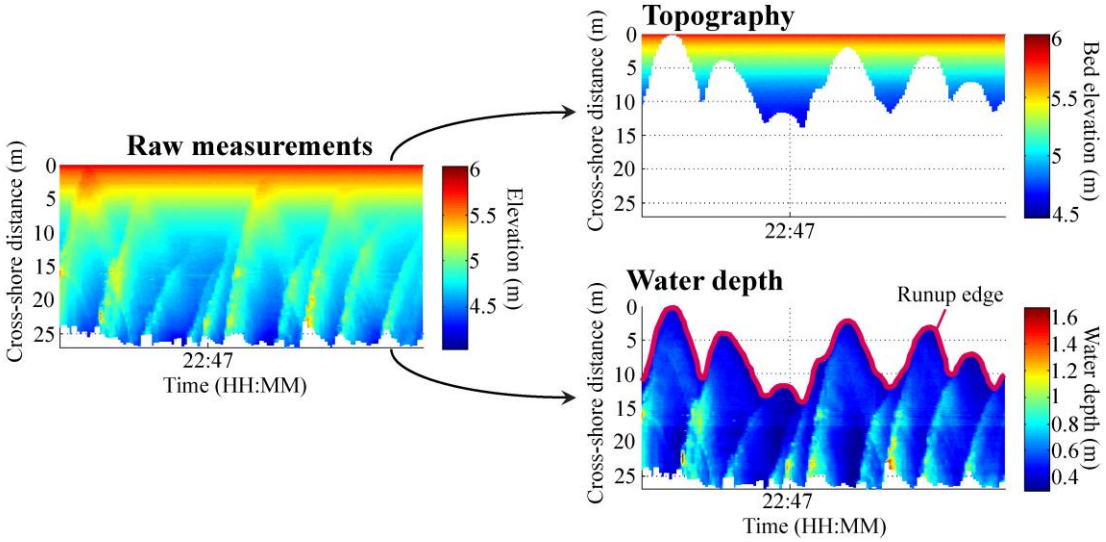

Figure 3. Raw measurements obtained from the laser-scanner (left panel) and the two types of time-series obtained after the data processing: 1) continuous topographic measurements (top right panel) and 2) swash hydrodynamics (bottom right panel).

Results

Wave (offshore) and tide measurements obtained during the field experiments at each site are presented in Figure 4. At Chesil beach, measurements were performed during a single tide cycle, covering an energetic SW (wave direction normal to the shoreline orientation) swell event with the offshore wave buoy recording waves with significant wave height (H_s) of approximately 2.5 m and peak period (T_p) around 10 seconds (Figure 4). A similar SW swell event, with slightly longer wave periods (T_p were between 10 and 13 s) and less steep waves, was recorded at Loe Bar during three tide cycles. At Hayling Island an extreme wind event (with gusts above 150 Km/h – measured at the Isle of Wight) with south direction was responsible for the generation of 3.5 m (H_s) waves with wave periods between 10 and 20 seconds, during which it two tide cycle of measurements were performed. Finally at Seascale one tide cycle was measured during a wave event with average offshore H_s of 3 m and T_p of 8 seconds (Figure 4).

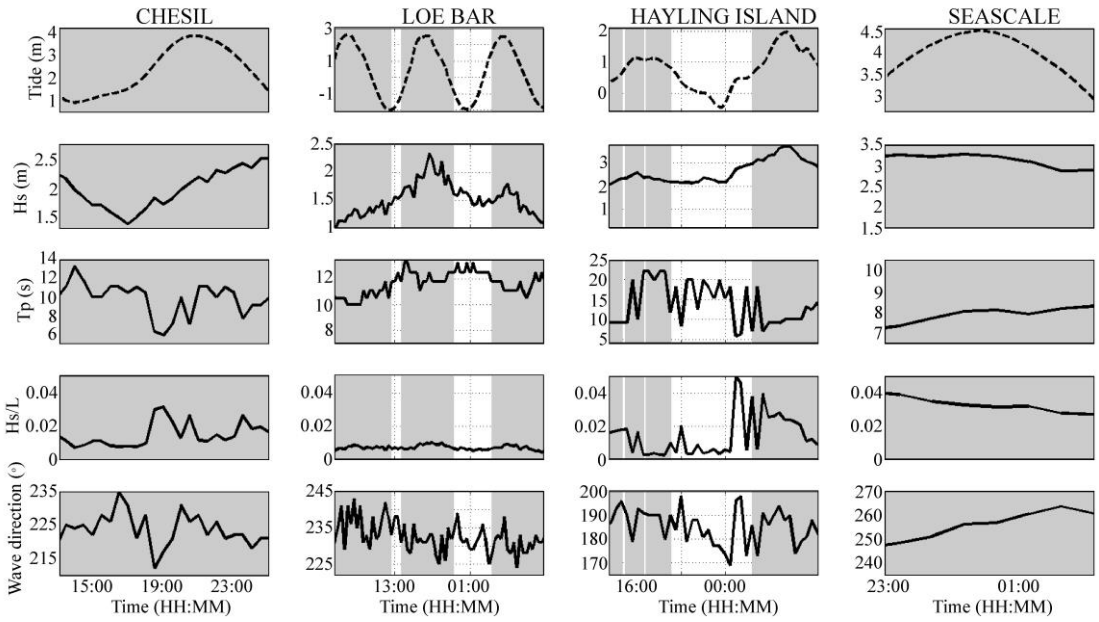

Figure 4. Tide height relative to ODN datum (black dashed line), offshore (black line) wave conditions during the field experiments; gray areas represent the time window when the laser-scanner was collecting data.

A comparison between offshore and inshore wave measurements was performed to assess the amount of wave dissipation occurred between offshore wave buoy and the inshore PT (Figure 5). In order to remove the tidal modulation effect present on part of the PT measurements only high tide measurements were used on this comparison.

From this comparison it is possible to verify that at Loe Bar the wave height at the lower beachface was higher or proportional to the offshore measurements, while at Seascale and Hayling Island a significant reduction of the wave height was observed on the inshore PTs measurements (Figure 5).

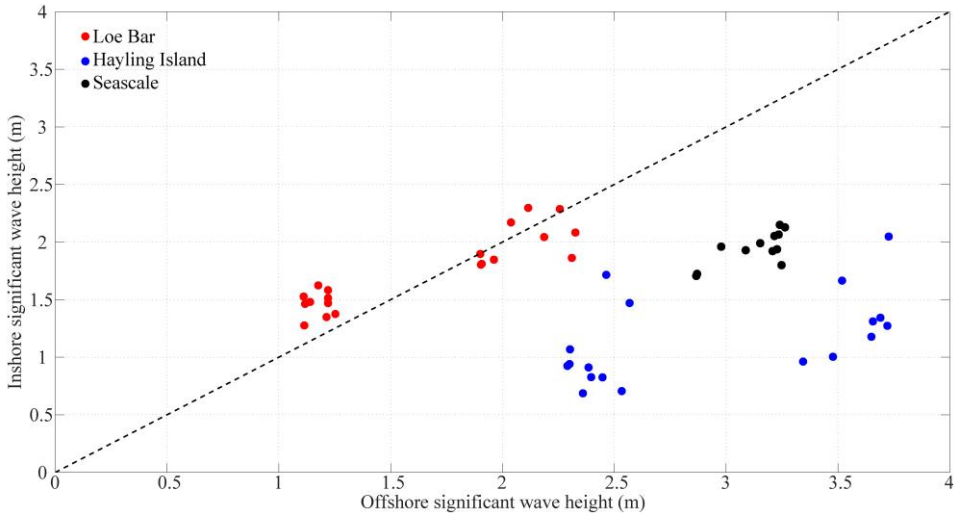

Figure 5. Scatter diagram of the offshore significant wave height measurements versus the inshore significant wave height measurements for all the sites.

Data analysis

Swash hydrodynamics measured by the laser-scanner at the different sites were analysed through the calculation of the following statistical parameters from the runup elevation time-series (R): (1) 2% exceedance of the runup maxima ($R_{2\%}$, see Figure 6); and (2) swash flow velocity skewness ($<u^3>$) computed as:

$$\langle u^3 \rangle = \frac{\langle u^3 \rangle}{\langle u^2 \rangle^{1.5}} \qquad (1)$$

where u is the cross-shore instantaneous velocity of the runup edge, computed through the first derivative of the horizontal runup (R_x) time series (Figure 7).

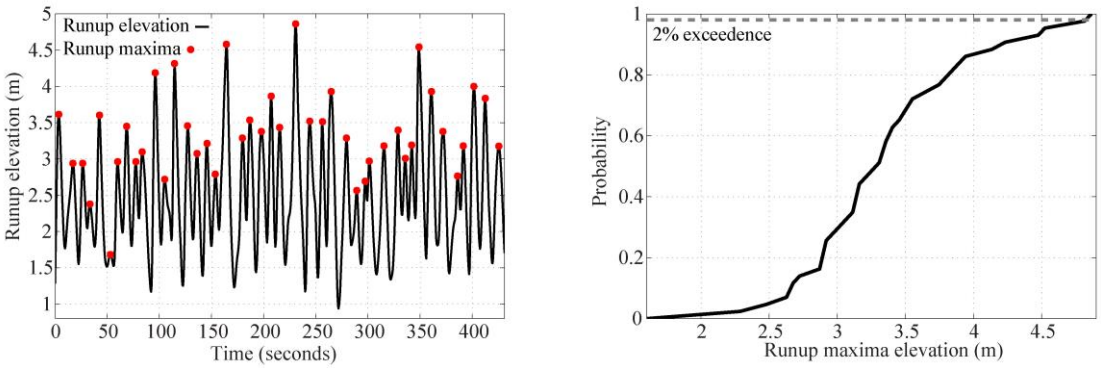

Figure 6. Example of a time series of runup elevation (R) with the identification of the runup maxima (red dots – left); from the cumulative PDF of the runup maxima is extracted the 2% of exceedance (right).

The concept of swash velocity skewness is explored here as a proxy of the swash flow dominance, and potential indicator of the sediment transport direction. For instance a positive skewed result indicates uprush flow dominance due to the dominance of short period and faster uprush flows in relation to longer and slower backwashes (Figure 7 – left). Negative skewed results on the other end indicate backwash flow dominance, with swash flows showing opposite characteristics to what was explained for the positive skewed flows (Figure 7 – right).

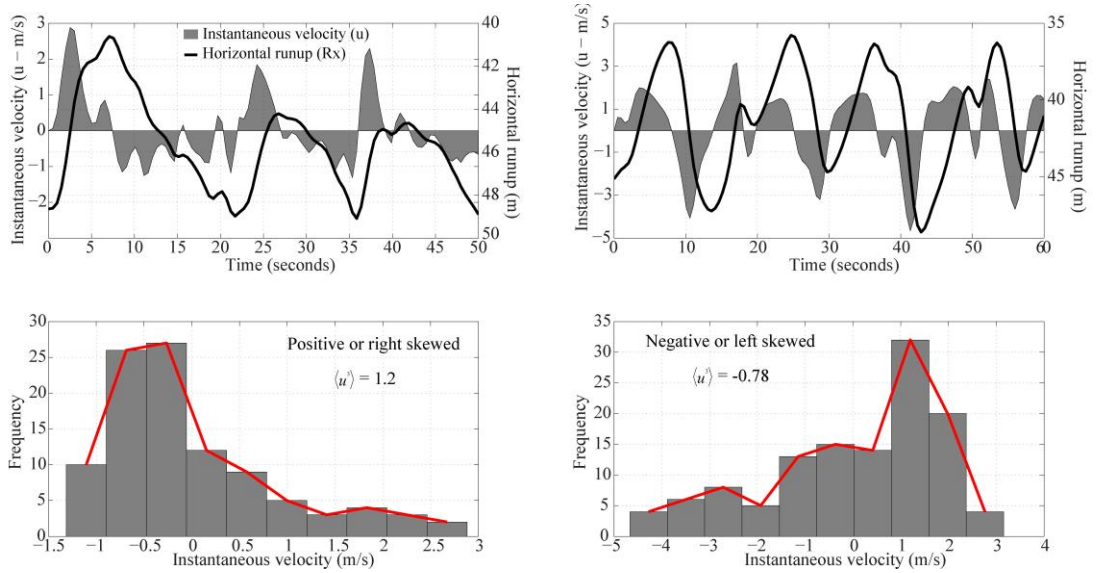

Figure 7. Two examples of swash velocity skewness results: left) time series of horizontal runup and respective instantaneous velocity (top), and resultant positive skewed velocity distribution (bottom); right) time series of horizontal runup and respective instantaneous velocity (top), and resultant negative skewed velocity distribution (bottom).

Wave dependence was removed from the $R_{2\%}$ by normalizing by the significant offshore wave height H_s. The morphodynamic status of the swash zone was determined using the surf-scaling parameter (Guza and Inman, 1975), ε:

$$\varepsilon = \frac{\pi^2 H_s}{g T_p \tan^2 \beta} \qquad (2)$$

where tanβ is the is the beach gradient across the "active" region of the beachface (between the runup and rundown limits) and g is gravity.

Swash morphological response was analysed by computing the cumulative vertical difference between consecutive beach profiles measured with the laser-scanner and the beach gradient (slope of the region constrained by the upper runup and lower rundown limit). All hydrodynamic and morphological parameters were computed for continuous segments of 15 minutes of data

Swash hydrodynamics

Time series of ε, $<u^3>$ and $R_{2\%}$ for all sites under different wave conditions are presented in Figure 8. For all sites the surf scaling was computed using continuous updated beach face slope (retrieved from the laser-scanner measurements) and offshore wave conditions, and results (Figure 8, second row) show that the swash zone of the PG and CSG beaches predominantly represent reflective or low intermediate regimes, while the MSG beach represent intermediate and dissipative regimes. Linked to these contrasting morphodynamics regimes presented by the different types of coarse-grained beaches are the wave dissipation processes on the swash zone. Field observations of the wave breaking in the swash zone (photos – see Figure 8, first row) highlight the differences between the sites: at PG beaches the absence of a alongshore bar and steep beach face slopes promote plunging breakers and therefore conditions for wave reflection; at CSG beach the flat intertidal terrace on the lower foreshore promoted

the dissipation of an important part of the offshore waves creating intermediate conditions during the peak of the storm; while at MSG beach the combination of a large surf zone (that dissipates most of the offshore waves) and gentle beach face slope produce a very dissipative swash zone (Figure 8).

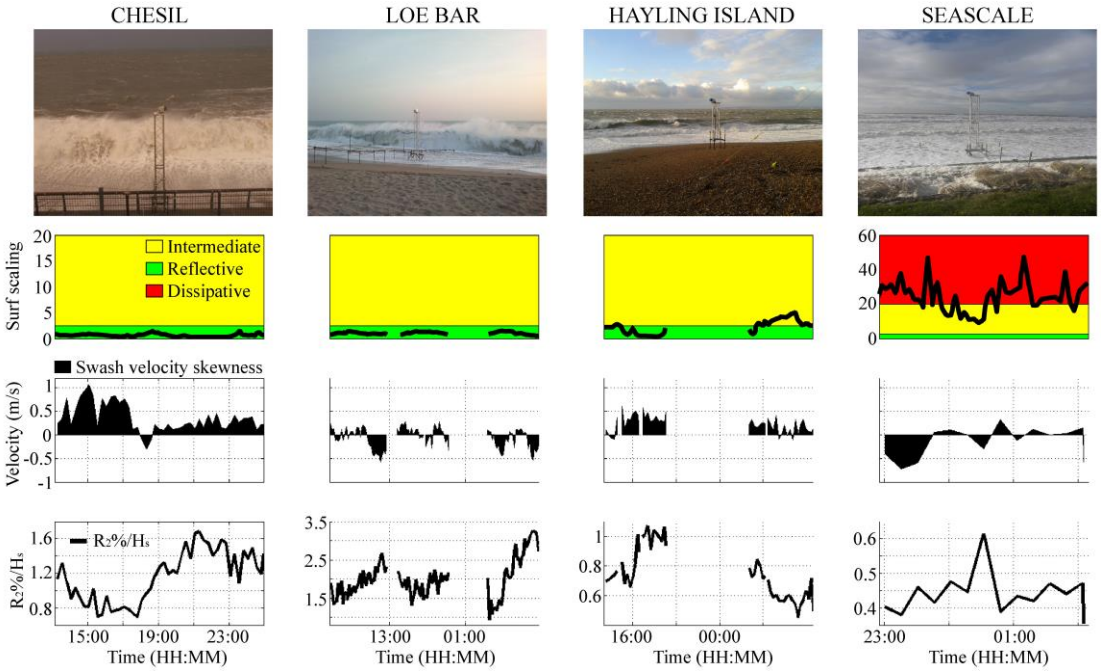

Figure 8. Field photos showing the wave breaking type for the different study sites (top panels); surf scaling (second row of panels), swash flow skewness (third row of panels), and 2% exceedence of the runup maxima (bottom panels), computed for all the sites.

The swash flow asymmetry was assessed through the velocity skewness $<u^3>$ and results show that coarser foreshores (Chesil and Hayling Island) show the highest asymmetries with a clear dominance of onshore flow asymmetry (positive $<u^3>$ values - Figure 8, third row). On the fine PG (Loe Bar) and MSG (Seascale) beaches the values for $<u^3>$ showed significant variability, indicating alternating onshore and offshore flwo asymmetry (Figure 8).

Extreme vertical runup, calculated here through the $R_{2\%}$ and normalized by the offshore significant wave height (H_s), shows that the highest runup levels were observed at Loe Bar, followed by Chesil, Hayling Island and finally Seascale (Figure 8, fourth row). Interestingly, for the three tides measured at Loe Bar the highest vertical runup excursions occurred during the ebb phase. Similar behaviour was observed at Hayling Island, but only during the first tide cycle of measurements (Figure 8), while at the other sites no clear relationship with the tide phase was found.

Swash morphological response

To evaluate the morphological response of the different coarse-grained beaches, the cumulative topographic changes and the beach face gradient were determined (Figure 9). Interpretation of these results reveals that PG beaches are characterised by an asymmetrical morphological response during the tide cycles, while for the CSG and MSG beaches the changes are persistent along the entire tide cycle (Figure 9, first row of panels).

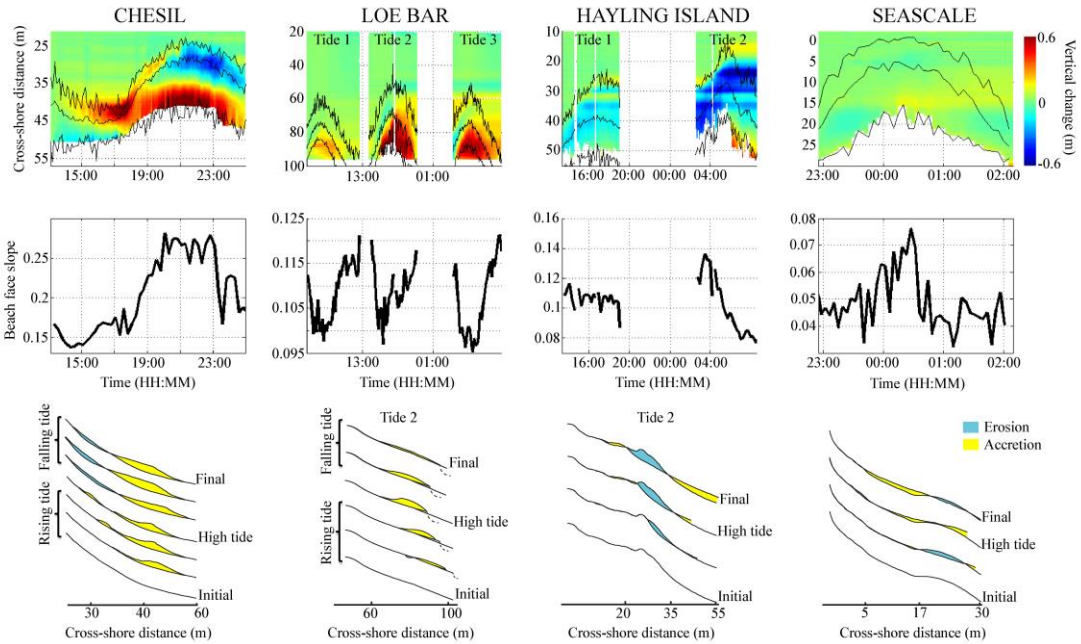

Figure 9. Contour plots showing the cumulative topographic changes calculated from the laser-scanner observations (top panels) with the overlap of the maximum and mean runup and minimum backwash position (black lines); beach face gradient (second row of panels); and a sketch of the representative morphological changes observed during a tide cycle (lower panels).

On both PG beaches the rising tide is characterized by dominant onshore sediment transport, with the development and onshore translation of a step deposit (Figure 10) (Poate et al., 2013; Almeida et al. *in press*). During the falling tide the step deposit gradually moves offshore shifting the dominant sediment transport direction towards offshore (Figure 9). On the CSG beach the present observations showed persistent erosion, during the two tide cycles, on the beach face and berm, with the accumulation of the eroded sediment on the lower beach (Figure 9).

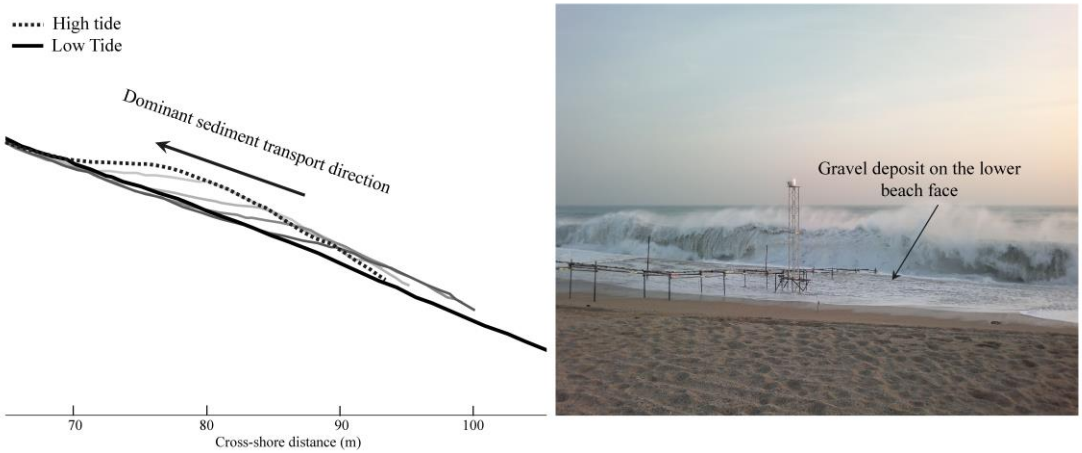

Figure 10. Several stages of development and onshore translation of the beach step deposit observed at Loe Bar during the most energetic tide cycle. Field photo (right) shows the shape of the deposit near high tide.

The morphological changes observed at MSG beach were relatively small compared with the other sites and showed persistent erosion on the lower beach face accompanied by accumulation on the upper part of the profile (Figure 9).

As a result of the significant morphological changes observed on these different coarse-grained beaches, the beach face slope also experienced important modifications during the tide cycle. On the PG beaches, the changes in the beach face gradient observed during the tide cycle were different,

despite the similarity in morphological response. At Loe Bar (fine PG beach) the development and onshore translation of the step deposit during the rising tide was associated with the reduction of the beach face slope, while at Chesil (coarse PG) beach face steepening was observed during the rising tide (Figure 9). During the falling tide, and with the removal of the step deposit, the trend was reversed: steepening of the beach face on the fine PG beach and a reduction in the beach face on the coarse PG beach (Figure 9).

On the CSG beach the beach face gradient progressively decreased over the two monitored tidal cycles, with the most energetic second tide showing the largest amount of variation (Figure 9). On the MSG beach, despite the small morphological changes observed, the variability in the beach face slope was significant (approximately 0.05 – see Figure 9) over the tide cycle. Results show an asymmetrical pattern of variation with the rising tide characterized by a steepening and the falling tide by a lower beach face gradient.

Morphological response and hydrodynamics

To compare and contrast the runup characteristics of the different beaches and place them within a morphodynamics framework, the normalised extreme runup was plotted against the surf scaling parameter (Figure 11). It is evident that the lower runup elevations are linked to the dissipative MSG swash zone, while the higher runup values are linked to the reflective PG beaches. In between these data clusters is the CSG beach which under (high tide) reflective conditions behaves like a PG beach, but under (low tide) intermediate conditions is characterised by lower runup excursions (Figure 11).

Under similar reflective regimes the two PG beaches represent significantly different values of the normalised extreme vertical runup, with the fine PG (Loe Bar) showing much higher values than the coarse PG (Chesil). This indicates the vertical runup is not only affected by the surf scaling parameter, and that additional processes are implicated.

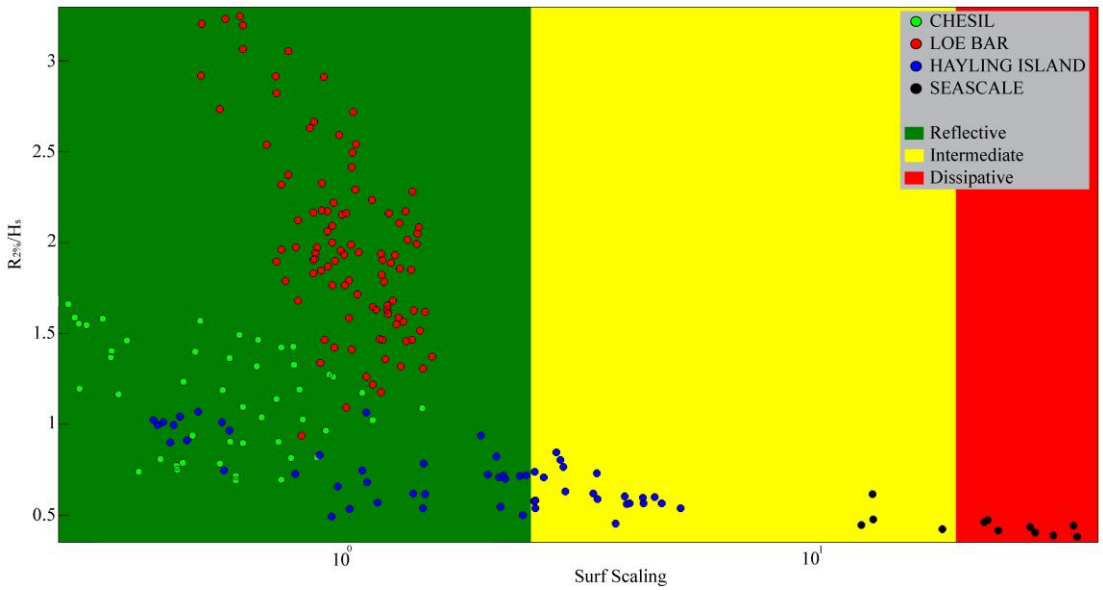

Figure 11. Scatter diagram of the surf scaling parameter versus the extreme runup ($R_{2\%}/H_s$) for all the measurements performed at each site. The circles with different colors represent the different sites (green – Chesil, red – Loe Bar, blue – Hayling Island and black – Seascale), and the background colors represent the different morphodynamics regimes (cream – reflective, blue – intermediate and gray – dissipative).

Discussion

In the initial section of this work the dissipation of the offshore waves in the surf zone was assessed by comparing the offshore and inshore wave measurements, and a clear difference on surf zone dynamics was noticed between the different coarse-grained beaches. Field observations showed that the PG beaches (Chesil and Loe Bar) develop very narrow surf zones with waves dissipating most of their energy on the beach step, a relatively small morphological feature at the base of the foreshore that forms a submerged break in slope at the base of the swash zone and which appears to adjust to neashore hydrodynamics regime (e.g., Hughes and Cowell, 1987). The beach step on PG beaches acts in an analogous way to a nearshore bar on sndy beaches by dissipating incident wave energy (Buscombe and

Masselink, 2006); however, due to the very small distance between the beach step and swash zone a large amount of wave energy still propagates into the swash zone, and for this reason the inshore wave measurements were similar or higher than the offshore wave measurements. Different surf zone mechanisms occur when the beach profile presents a wide and very dissipative intertidal terrace, such as at Seascale (the MSG beach). Here, most of the offshore wave energy is dissipated across a wide surf zone before reaching the swash zone; therefore, a significant reduction in the wave height was observed when comparing the inshore PT data with the offshore wave measurements.

Hayling Island (the CSG beach) occupies an intermediate position. Characterised by a small beach step and a narrow intertidal terrace, it develops a slightly wider surf zone than the PG beaches, but narrower and less dissipative than the MSG beach. Here, the reduction in the wave height from offshore to inshore was also significant, and with a similar ratio to that observed for Seascale. Nevertheless, it is important to take in consideration that the position of the inshore PTs at these two sites was different. At Seascale, the inshore PT was located on the lower beach face, and during mid to high tide was measuring the surf zone processes, while the inshore PT deployed at Hayling Island was located on the mid beach face and during mid to high tide was measuring mostly swash zone processes (e.g. swash bores).

The different surf zone dynamics promote different boundary conditions for the swash zone and this has a direct effect on the sediment transport processes. The character of wave breaking is significant in the context of sediment transport, because the amount of turbulence reaching the bed depends on wave (breaker) type. For instance, the momentum impact of plunging breaker vortices on the sea bed mobilizes larger amounts of sediment than spilling breaker (Aagard and Hughes, 2010). This aspect is particularly important on these different coarse-grained beaches where important differences on the dominant breaker type were identified. At PG beaches the dominant plunging breakers are believed to represent a key mechanism to entrain sediment from the step into the water column (e.g. Brocchini and Baldock, 2008) that is subsequently advected into the uprush flow and transported onshore before settling down at flow reversal.

During the rising tide, the onshore translation of the breaking point together with the unsaturated beach face promotes onshore sediment transport and an important reduction of backwash flows due to the large amount of infiltration during the uprush. These processes are believed to contribute to the development of the beach step deposit during the rising tide (Kulkarni et al., 2004; Almeida et al., *in press*), while on the falling tide the offshore shift of the breaking point decreases the advected sediment into the uprush and creates a deficit in onshore sediment transport and favouring offshore sediment transport through the backwash. The dynamic equilibrium between beach morphology and hydrodynamics provides to PG beaches an efficient mechanism of natural protection, but seems absent on the other types of coarse-grained beaches.

On the MSG beach, the presence of a very dissipative surf zone seems to be a fundamental aspect of differentiation from the other sites, since most of the offshore wave energy is dissipated before reaching the swash zone. When waves reach the low gradient swash zone they dissipate their energy with spilling breakers, and these tend to generate less turbulence on the bed (Christensen and Deigaard, 2001) and therefore less sediment is added to the water column and transported. This is reflected in the small magnitude of morphological changes observed at Seascale, despite the energetic offshore wave conditions.

On the CSG beach, and despite the presence of a small beach step, the mechanism of step translation found on the PG beaches did not occur. The persistent erosion of the upper beach face and berm crest during energetic wave conditions on CSG beach has been observed elsewhere (e.g., Pontee et al., 2004), but continuous measurement of the morphology and swash hydrodynamics on this type of beaches during energetic conditions are absent in the literature. Present observations showed that the narrow intertidal sandy terrace on the CSG beach dissipates an important amount of the offshore wave energy, which promote waves to break before reaching the swash zone. Therefore the levels of energy on the swash zone and the potential onshore sediment transport decreases, favouring offshore sediment transport through the backwash. This process neglects any longshore contributions to the sediment transport, which might be important aspect mainly when offshore waves approach swash with oblique angles.

The scatter diagram of Figure 11 shows that for lower intermediate and reflective regimes, the swash zones of coarse-grained beaches represent the highest normalised vertical runup values. Nevertheless, under similar morphodynamic regimes, the fine PG beach is characterised by considerably higher runup

values than the coarse PG and CSG beaches. This means that the surf scaling parameter is not sufficient to explain the variability in vertical runup on these different coarse-grained swash zones.
A possible explanation for the difference between vertical runup characteristics can be attributed to the sediment size, as this is the most significant difference between the swash zones of these three sites. While the swash zone of the coarse PG and CSG beach are composed by coarse gravel, the fine PG beach is mostly composed by fine gravel and some coarse sand. With coarser grains the permeability and roughness of the bed increases, increasing the infiltration (Masselink and Li, 2001) and friction forces (Horn and Li, 2006), reducing the velocity and runup elevation.
The present results of the swash flow velocity skewness $<u^3>$ show that the coarser swash zones (Chesil and Hayling Island) are characterized by strong asymmetrical swash flows (with onshore flow dominance - positive skewness). These results are in agreement with Masselink and Li (2001) that, through a processed-based model, demonstrated the swash flow asymmetry increases and runup elevation decreases with larger values of hydraulic conductivity.
Using the $<u^3>$ as a proxy of these two dissipation factors (infiltration and friction) the present results suggest that the higher vertical runup excursions observed at Loe Bar (fine PG) are a result of the relative smaller permeability and roughness, comparing with the coarser swash zones of Chesil and Hayling Island.
Infiltration and loss due to friction are, however, not the only factors affecting the runup heights on coarse-grained beaches and other aspects such as the wave steepness, might be of great importance. The present observations indicate that the waves conditions measured at Loe Bar presented higher periods than the waves observed at Chesil, indicating that this factor might be contributing for such a difference on the results.
Despite this suggestion, further analysis should be performed in order to explore and quantify the relationship between the infiltration\friction properties of different coarse-grained swash zones and the importance of wave steepness on the vertical runup.

Conclusion

A 2D laser-scanner was deployed on four different coarse-grained beaches (two PG beaches, one CSG and one MSG beach) to measure swash zone hydrodynamics and morphological changes during energetic wave conditions. Contrasting morphological responses were observed on the different coarse-grained beaches as a result of the different swash\surf zone dynamics. PG beaches with a narrow surf zone on the edge of the swash, presented an asymmetric morphological response during the tide cycle (accretion during the rising and erosion during the falling tide) as a result of beach step adjustments to the prevailing hydrodynamics. On the MSG beach, the morphological response was not significant due to the very dissipative surf zone, while at the CSG beach significant erosion of the beach face and berm was observed during the entire tide cycle as a result of the absence of dissipative surf zone and beach step dynamics. Although an important part of the runup variability was explained by the surf scaling parameter, present results indicate that dissipation through permeability\bed friction due to the different sediment size and wave steepness may be an important parameter to take in consideration when estimating vertical runup excursions.

Acknowledgements

The work described in this publication was supported by the EPSRC projects ARCoES (Adaptation and resilience of the UK energy system to climate changes; EP/1035390/1) and NUPSIG (New Understanding and Prediction of Storm Impacts on Gravel beaches; EP/H040056/1, in partnership with the Channel Coastal Observatory (CCO), HR Wallingford and The Environment Agency). The authors of this work would like to thank the support provided by Peter Ganderton in the setup of the laser-scanner, and Erwin Bergsma, Andrea Ruju for field assistance during the field experiments.

REFERENCES

Aagaard, T., Hughes, M.G., 2010. Breaker turbulence and sediment suspension in the surf zone. *Marine Geology*, 271, pp. 250-259.

Almeida, L.P., Masselink, G., Russell, P., Davidson, M., Poate, T., McCall, R., Blenkinsopp, C., Turner, I.L., 2013. Observations of the swash zone on a gravel beach during a storm using a laser-scanner (Lidar). Journal of Coastal Research, 65, 636-641.

Almeida, L.P., Masselink, G., Russell, P., Davidson, M., 2014. Observations of gravel beach dynamics during high energy wave conditions using a laser scanner. *Geomorphology*, DOI: 10.1016/j.geomorph.2014.08.019.

Austin, M.J., Masselink, G., 2006. Observations of morphological change and sediment transport on a steep gravel beach. *Marine Geology*, 229, 59–77.

Austin, M.J., Buscombe, D., 2008. Morphological change and sediment dynamics of the beach step on a macrotidal gravel beach. *Marine Geology*, 249, 167–183.

Blenkinsopp, C.E., Mole, M.A., Turner, I.L., Peirson, W.L., 2010. Measurements of the time-varying free-surface profile across the swash zone obtained using an industrial lidar. *Coastal Engineering*, 57, 1059-1065.

Blenkinsopp, C.E., Turner, I.L., Allis, M.J., Peirson, W.L., Garden, L.E., 2012. Application of LiDAR technology for measurement of time-varying free-surface profiles in a laboratory wave flume. *Coastal Engineering*, 68, 1-5.

Brodie, K.L., Slocum, R.K., McNinch, J.E., 2012. New insights into the physical drivers of wave runup from a continuously operating terrestrial laser scanner. *Final Proceedings of Ocean's 12*, Virginia, U.S.A., pp. 1-8.

Brocchini, M., Baldock, T.E., 2008. Recent advances in modeling swash zone dynamics: influence of surf–swash interaction on nearshore hydrodynamics and morphodynamics. *Reviews of Geophysics*, 46, RG3003.

Buscombe, D., Masselink, G., 2006. Concepts in gravel beach dynamics. *Earth Science Reviews*, 79, 33–52.

Carr, A.P. (1969) Size grading along a pebble beach: Chesil Beach, England. *Journal of Sedimentary Petrology*, 39, 297–311.

Carr, A.P., 1983. Shingle beaches: aspects of their structure and stability. *Shoreline protection. Proceedings of Shore Protection*, A Conference Organised by the Institution of Civil Engineers. University of Southampton, Thomas Telford, pp. 69–76

Carter, R.W.G., Orford, J.D., 1984. Coarse clastic barrier beaches: a discussion of the distinctive dynamic and morphosedimentary characteristics. *Marine Geology*, 60, 377–389.

Carter, R.W.G., Orford, J.D., 1993. The morphodynamics of coarse clastic beaches and barriers: a short- and long-term perspective. Journal of Coastal Research, 15, pp. 158-179.

Christensen, E.D., Deigaard, R., 2001. Large eddy simulation of breaking waves. *Coastal Engineering* 42, 53–86.

Guza, R.T., Inman, D.L., 1975. Edge waves and beach cusps. Journal of Geophysical Research, 80, pp. 2997-3012.

Horn, D.P., Li, L., Holmes, P., 2006. Measurement and modelling of gravel beach groundwater response to wave run-up: effects on beach profile changes. Journal of Coastal Research, 22, pp. 1241-1249.

Hughes, M.G., Cowell, P.J., 1987. Adjustment of reflective beaches to waves. *Journal of Coastal Research*, 3, 153–167.

Ivamy, M.C., Kench, P.S., 2006. Hydrodynamics and morphological adjustment of a mixed sand and gravel beach, Torere, Bay of Plenty, New Zealand. *Marine Geology*, 228, 137–152.

Jennings, R., Schulmeister, J., 2002. A field based classification scheme for gravel beaches. *Marine Geology*, 186, 211-228.

Kirk, R. M., 1970: Swash zone processes: An exami-nation of water motion and the relations between water motion and foreshore response on some mixed sand and shingle beaches, Kaikoura, New Zealand. *Ph.D. thesis*, Dept Geography, Univ. Canterbury, Christchurch, New Zealand.

Kulkarni, C.D., Levoy, F., Montfort, O., Miles, J., 2004. Morphological variations of a mixed sediment beachface (Teignmouth, UK). *Continental Shelf Research*, 24, 1203–1218.

Mason, T., Voulgaris, G., Simmonds, D.J., Collis, M.B., 1997. Hydrodynamics and sediment transport o composite (mixed sand/shingle) beaches: a comparison. *Coastal Dynamics '97*. ASCE, pp. 48–57.

Moses, C.A., Williams, R.B.G., 2008. Artificial beach recharge: the south-east England experience. Zeitschrift für Geomorphologie 52, pp. 107–124.

Masselink, G., Russell, P., Blenkinsopp, C.E., Turner, I.L., 2010. Swash zone sediment transport, step dynamics and morphological response on a gravel beach. *Marine Geology*, 274, 50–68.

Masselink, G., Li, L., 2001. The role of swash infiltration in determining the beachface gradient: a numerical study. *Marine Geology*. 176, 139–156.

Orford, J.D., Carter, R.W.G., 1984. Mechanisms to account for the longshore spacing of overwash throats on a coarse clastic barrier in southeast Ireland. *Marine Geology*, 56, 207–226.

Osborne, P.D., 2005. Transport of gravel and cobble on a mixed sediment inner bank shoreline of a large inlet, Grays Harbor,Washington. *Marine Geology*, 224, 145–156.

Pedrozo-Acuña, A., Simmonds, D.J., Otta, A.K., Chadwick, A.J., 2006. On the cross-shore profile change of gravel beaches. *Coastal Engineering*, 53 (4), 335–347.

Poate, T., Masselink, G., McCall, R., Russell, P., Davidson, M., Turner, I.L., 2013. Field measurements of gravel beach response during storm conditions. *Marine Geology*, 342, 1-13.

Pontee, N.I., Pye, K., Blott, S.J., 2004.Morphodynamic behaviour and sedimentary variation of mixed sand and gravel beaches, Suffolk, UK. *Journal of Coastal Research*, 20 (1), 256–276.

Puleo, J., 2004. Hydrodynamics and sediment transport in the inner surf and swash zones.PhD dissertation, University of Florida, U.S.A.

Van Wellen, E., Chadwick, A.J., Mason, T., 2000. A review and assessment of longshore sediment transport equations for coarse grained beaches. Coastal Engineering 40, pp. 243–275.

SICK, 2009. LD-OEM1000 to 5100 Laser Measurement System – operating manual. SICK AG Waldkirch, Germany.

Whitecombe, L.J., 1996. Behaviour of an artificially replenished shingle beach at Hayling Island, UK. Quarterly Journal of Engineering Geology, 29, pp. 265-271.